

A phenomenological model of multiple particle production and highest energy air showers.

A. Ohsawa¹, E. H. Shibuya², and M. Tamada³

¹Institute for Cosmic Ray Research, University of Tokyo, Kashiwa, Chiba, 277-8582 Japan.

²Instituto de Fisica Gleb Wataghin, Univ. Estadual de Campinas, 13083-970 Campinas, São Paulo, Brasil.

³Faculty of Science and Technology, Kinki University, Higashi-Osaka, Osaka, 577 Japan.

Abstract. The energy distribution of produced particles in multiple particle production, which is formulated empirically based on the direct observation data by accelerator and cosmic-ray experiments, shows violation of the Feynman scaling law with decreasing inelasticity at high energies. We show that the extrapolation of the formulated distribution does not describe the highest energy ($\sim 10^{20}$ eV) air showers. We also discuss how large the ambiguity is in the energy determination of highest energy air showers, due to limited information on nuclear interaction characteristics at high energies.

1 Introduction

We formulated empirically the energy distribution of produced particles in multiple particle production, based on the data of direct observation by accelerator and cosmic-ray experiments in the energy region $10^{12} \sim 10^{14}$ eV. (Ohsawa et al., 2000)

The formulated energy distribution shows that the Feynman scaling law, which is shown to be valid in the energy region below $\sqrt{s} = 63$ GeV, is violated appreciably both in the central region and in the forward region at high energy. That is, the particle production is enhanced in the central region and suppressed in the forward region. And the suppression in the forward region is stronger than the enhancement in the central region. Consequently the total inelasticity $\langle K \rangle$ becomes smaller than 0.5 appreciably at high energy. It is also shown that the nuclear interaction models, which are assumed in the recent calculations to simulate the cosmic-ray diffusion in the atmosphere, are not compatible with the formulated energy distribution.

In the present paper we discuss whether the formulated energy distribution is compatible or not with the data of extremely high energy ($\sim 10^{20}$ eV) air showers. The energy dependence of nuclear interaction characteristics appears in most distinct way at these energies.

Correspondence to: A. Ohsaw (ohsawa@icrr.u-tokyo.ac.jp)

2 Diffusion of Cosmic rays in the atmosphere.

2.1 Air showers

A high energy primary cosmic-ray proton, incident upon the top of the atmosphere, makes a nuclear collision with an atmospheric nucleus, and many particles — one surviving particle and a number of produced particles — are produced through the collision. The surviving particle, either a proton or a neutron, repeats inelastic collisions in the atmosphere. The inelastic cross section of the nucleon-air collision increases with the incident energy.

The produced particles are assumed to be pions. The energy distribution of produced pions is substituted by that of $N - N$ collision, which is formulated by us (Ohsawa et al., 2000), because the effect of the air nucleus target appears only in the backward region.¹ The charged pions among the produced pions make nuclear collisions in the atmosphere again. The collision mean free path of charged pions has the same energy dependence as that of nucleon. We neglect decays of charged pions into muons.

The multiple particle production, induced by a charged pion, has essentially the same characteristics as the one by a nucleon, which is confirmed within the errors of the experimental data in low energy region. (Gaisser et al., 1978)

That is, the final state of the collision consists of one surviving pion and produced pions whose energy distribution is the same as the one of proton collision. The differences are that the inelastic cross section of pion is smaller than that of proton, and that the surviving pion has a probability to be a neutral pion (called the 'charge exchange' process).

The neutral pions among the produced pions and those through the charge exchange process decay into γ -rays which produce a number of electromagnetic component, electrons and photons, via electromagnetic cascade process.

¹The diffusion of cosmic rays in the atmosphere is governed by the high energy particles, produced in the forward region.

Table 1. Energy dependences of the scaling violation parameters

Model	α	α'	$\langle K \rangle$	Remark
Model-0	0	0	0.5	
Model-1	0.105	0.105	0.5	
Model-2	0.105	0.210	$0.5(E_0/A)^{-0.105}$	the best-fit

2.2 Assumptions for elementary processes

Following the above scenario we formulate the elementary processes.

(1) Inelastic collision mean free path

We formulate the energy dependence of the mean free paths of $N - air$ and $\pi - air$ collisions in the following way. (Nam et al., 1983), (Hara et al., 1983), (Dyakonov et al., 1987)

$$\lambda_N(E_0) = \lambda_N \left(\frac{E_0}{B} \right)^{-\beta} \quad \lambda_\pi(E_0) = \lambda_\pi \left(\frac{E_0}{B} \right)^{-\beta} \quad (1)$$

$$(\lambda_N = 80.0 \text{ g/cm}^2, \lambda_\pi = 113 \text{ g/cm}^2, \beta = 0.056)$$

(2) Energy distribution of produced particles

The energy distribution of produced *charged* particles in multiple particle production is formulated in our paper. (Oh-sawa et al., 2000) In the laboratory system it is

$$\varphi(E_0, E) dE = D \left(\frac{E_0}{A} \right)^\alpha \left[1 - \left(\frac{E_0}{A} \right)^{\alpha'} \frac{E}{E_0} \right]^d \frac{dE}{E} \quad (2)$$

$$(A = 2.0 \times 10^2 \text{ GeV}, D = 1.67, d = 4.0)$$

where E_0 is the energy of the incident particle. The parameters α and α' are tabulated in Table 1. The values of Model-2 are the best-fit to the experimental data, and Model-0 and Model-1 are for reference.

(3) Inelasticity

According to eq.(2) the average total inelasticity is given by

$$\langle K \rangle \equiv \frac{3}{2} \int_0^{E_0} E \varphi(E_0, E) dE = 0.5 \left(\frac{E_0}{A} \right)^{\alpha - \alpha'}$$

That is, the average inelasticity decreases with the incident energy for Model-2.

We assume that the inelasticity K is distributed uniformly between 0 and 2 $\langle K \rangle$ (≤ 1.0). The distribution has the average value of the inelasticity $\langle K \rangle$.

(4) Charge exchange probability of the surviving pion is assumed to be $b = 0.3$.

3 Air shower size

As can be seen in Appendix A, one can calculate the air shower size N_e if one can solve the diffusion equations for nucleon and pion components. It is not simple, however, to solve them taking all the processes, mentioned above, into account simultaneously. Therefore we discuss the effects of

Table 2. Cases to be discussed

Case	α and α' in eq.(2)	Cross section	Remark
A	0 (the scaling law)	$\beta = 0$ (constant)	$b = 0$ and $b = 0.3$
B	0 (the scaling law)	$\beta = 0.056$ (increasing)	
C	0.105 (the law violated)	$\beta = 0$ (constant)	Model-1
D	0.105 (the law violated)	$\beta = 0$ (constant)	Model-2

respective processes one by one. That is, we calculate the cases, tabulated in Table 2, and discuss the ratio between the air shower size of each process and that of the case A.

Fig. 1 shows the transition curve of the air shower size of the case A for the primary proton with the energies $E_0 = 10^{18}$, 10^{19} , and 10^{20} eV. (See Appendix A.) One can see in the figure that the air showers of 10^{20} eV are at the maximum development at sea level and that the relation $E_0/N_e \simeq 2.0$ (GeV) holds approximately, irrespective of the primary energy E_0 .

The effect of the charge exchange process is examined, too, assuming the probability $b = 0.3$. The effect is almost constant over the atmospheric depth, amounting 13 %, as can be seen in Fig. 2. The approximately constant effect over the depth can be explained by the facts; (1) that the probability b is included in the attenuation mean free path of pion component $\xi\mu_\pi(s)$ and in the coefficient of the pion term, in such ways that the attenuation of the air shower size becomes faster and that the size becomes larger, respectively, and (2) that the shower development before the shower maximum is governed by $e^{\xi_0\lambda_1(s)z}$ but not by $e^{\xi\mu_\pi(s)z}$. (See Appendix A.)

Fig. 2 shows the ratio of the air shower size between the cases B, C and D and the case A, tabulated in Table 2, at the primary energy $E_0 = 10^{20}$ eV. One can see the following in the figure.

- (1) Effect of the charge exchange process of the surviving pion is almost constant over the atmospheric depth, and amounts 13 %.
- (2) Effect of increasing cross section is large at high altitude, but is small at sea level. (This tendency can be seen by the analytic expression of the air shower size where the increasing cross section is taken into account.)
- (3) The effects of scaling violation, in Model-1 and in Model-2, have similar depth dependence, but the absolute values of them differ by five times.
- (4) Model-2 gives smaller air shower size, and the attenuation of the air shower size after the shower maximum is very slow due to the small value of inelasticity.
- (5) At sea level the air shower size is affected in the greatest manner by the difference of the nuclear interaction model, among the examined processes of nuclear interaction characteristics.

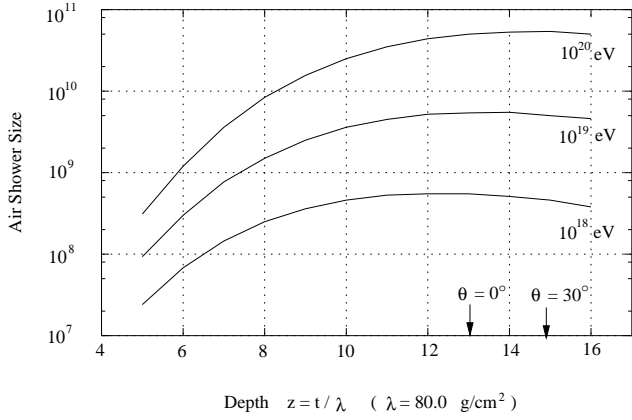


Fig. 1. Transition curve of the air shower size for the primary proton with the energy $E_0 = 10^{18}$, 10^{19} and 10^{20} eV, for Case A (Model-0 and constant cross section). The arrows indicate the depth of the sea level ($1,030 \text{ g/cm}^2$) for the air showers with the inclination $\theta = 0^\circ$ and 30° .

4 Summary and discussions

(i) Analytical expression is given for the air shower size, based on the formulated models of nuclear interactions. It enables us to discuss how the physical processes — the charge exchange of the surviving pion, increasing cross section of *hadron* – *air* collisions, and the energy distribution of produced particles — affect the air shower size. These processes are the major factors to govern the diffusion of high energy cosmic rays in the atmosphere. We obtained the following observations about the size of the extremely high energy air showers.

- (1) Effect of charge exchange process is almost constant ($\times 1.13$) over the whole depth in the atmosphere.
- (2) Effect of increasing cross section is large ($\times 2 \sim 3$) at mountain altitudes, but small ($\times 1.18$) at the sea level.
- (3) Effect of scaling violation of Model-1 is large ($\times 2 \sim 3$) at mountain altitudes, but small ($\times 1.23$) at sea level.
- (4) Effect of scaling violation of Model-2 is not negligible at any depth, *i.e.* $\times 0.6 \sim 0.4$ at mountain altitudes and $\times 0.22$ at the sea level.

(ii) The air shower size at sea level, expected by the present calculation, is tabulated in Table 3 for the incident proton of $E_0 = 10^{20}$ eV. In the table the effects of the charge exchange process and the increasing cross section are obtained by Fig. 2. To calculate the expected air shower size, to which the effects of charge exchange probability and increasing cross section are included, we multiplied all the factors because the factors are close to 1.0.

(iii) M. Nagano *et al.* examined the method of energy determination of extremely high energy air showers, employed by AGASA experiment, by the simulation code of CORSIKA (Capdevielle *et al.*, 1992)(with QGSJET model). And they reached the conclusion that the method works well for the highest energy air showers. (Nagano *et al.*, 1998) The simulation gives $N_e = 5.5 \times 10^{10}$ for the proton-induced air

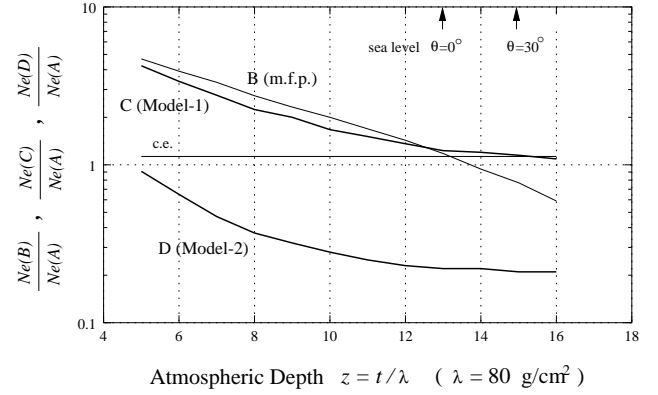


Fig. 2. Ratio of air shower size, $N_e(B)/N_e(A)$, $N_e(C)/N_e(A)$ and $N_e(D)/N_e(A)$, along the depth. The cases of A, B, C and D are tabulated in Table 2. The primary energy of a proton is 10^{20} eV.

showers of $E_0 = 10^{20}$ eV.² We can see the following points by comparing the value with those in Table 3.

- (1) The value by the simulation is between those of Model-1 and Model-2. In this sense our calculation and the simulation are consistent each other, because we saw in our paper (Ohsawa *et al.*, 2000) that the pseudo-rapidity density distribution by the QGSJET model is between those by Model-1 and Model-2.
- (2) If we take Model-1, the energy spectrum of highest energy air showers shifts to the left (lower energy side) by a factor 1.5.
- (3) If we take Model-2, which is the best-fit to the experimental data, the energy spectrum shifts to right (higher energy side) by a factor 3.7.

One can see that the energy distribution of produced particles has the largest effect on the size of extremely high energy air showers among the physical processes, discussed in this paper. Hence we have to specify the energy distribution of produced particles in multiple particle production in more detail, in order to confirm the extremely high energy cosmic rays exceeding 10^{20} eV.

(iv) The item (3) in the paragraph (iii) makes the puzzle of extremely high energy cosmic rays more serious.³ Therefore it may not be irrelevant to say that Model-2 does not describe the highest energy air showers. This examination is important because it is believed that the air shower size is a stable parameter to be unchanged by a slight difference of nuclear interaction characteristics.

Origin of this small size in Model-2 is due to the fact that Model-2, which is the best-fit to the present experimental data, predicts small inelasticity at high energies. For example, the value is as small as 0.2 even at $E_0 = 10^{16}$ eV. (Ohsawa *et al.*, 2000) According to our previous analysis of attenuation mean free paths of hadron and (e, γ) compo-

²We obtained $N_e = 5.5 \times 10^9$ for the proton-induced air showers of $E_0 = 10^{19}$ eV, from the figure in Ref. (Nagano *et al.*, 1998), and multiplied it by 10.

³The air showers with energy exceeding the GZK cut-off.

Table 3. Air shower size at sea level, expected by the models, for the incident proton of $E_0 = 10^{20}$ eV

	Model-0	Model-1	Model-2	CORSIKA
size*	5.0×10^{10}	6.2×10^{10}	1.1×10^{10}	
ratio to Model-0	($\times 1.0$)	($\times 1.23$)	($\times 0.22$)	
charge exchange	$\times 1.13$	$\times 1.13$	$\times 1.13$	
increasing cross section	$\times 1.18$	$\times 1.18$	$\times 1.18$	
size (expected)**	6.7×10^{10}	8.3×10^{10}	1.5×10^{10}	5.5×10^{10}

* without the processes of increasing cross section and the charge exchange.

** with the processes of increasing cross section and the charge exchange.

nents (Ohsawa and Sawayanagi, 1992), the inelasticity of $\langle K \rangle = 0.5$ is compatible with the experimental data in the energy region of $10^{14} \sim 10^{16}$ eV.

Appendix A Air shower size

Air shower size is defined as the total number of charged particles in the air shower, among which the electron component is dominant. Therefore we calculate only the electron component for the air shower size. It is given by

$$N_e(E_0, z) = \int_0^z dz' \int_0^\infty dE \Pi(E, 0, z - z') \times \left[\frac{\phi(s)}{s+1} F_N(E, z') + \xi \frac{\phi(s) + 2b \langle (1-K)^s \rangle}{s+1} F_\pi(E, z') \right]$$

where $F_N(E, z)$ and $F_\pi(E, z)$ are the number of nucleons and pions with energy E at the depth z . And $\Pi(E_0, 0, z)$ is the number of electrons ($E \geq 0$) under Approximation B.

In the case A we can solve the diffusion equations for nucleons and pions exactly, on the basis of the physical processes described in Section 2, and we have

$$N_e(E_0, z) = \frac{1}{2\pi i} \int \frac{ds}{s(s+1)} \left(\frac{E_0}{\epsilon} \right)^s L(s) \sqrt{s} K_{1,0}(s, -s) \times \phi(s) \left[\frac{e^{\mu_N(s)z} - e^{\xi_0 \lambda_1(s)z}}{\mu_N(s) - \xi_0 \lambda_1(s)} + \xi \frac{\phi(s) + 2b \langle (1-K)^s \rangle}{\mu_N(s) - \xi \mu_\pi(s)} \left\{ \frac{e^{\mu_N(s)z} - e^{\xi_0 \lambda_1(s)z}}{\mu_N(s) - \xi_0 \lambda_1(s)} - \frac{e^{\xi \mu_\pi(s)z} - e^{\xi_0 \lambda_1(s)z}}{\xi \mu_\pi(s) - \xi_0 \lambda_1(s)} \right\} \right]$$

where z is measured in the unit of λ_N . (*i.e.*, $\xi = \lambda_N/\lambda_\pi$, $\xi_0 = \lambda_N/X_0$) The integration is a complex one, originated

from the inverse Mellin transformation. The first line is related to the cascade functions, and the second and the third are to the π^0 production by nucleons and pions.

The terms $\mu_N(s)$, $\xi \mu_\pi(s)$ and $\xi_0 \lambda_1(s)$ are related to the attenuation of nucleons, pions and electrons, respectively.

$$\mu_N(s) = -1 + \langle (1-K)^s \rangle$$

$$\mu_\pi(s) = -1 + (1-b) \langle (1-K)^s \rangle + \phi(s)$$

$$\lambda_1(s) = (\text{by the cascade theory})$$

where $\phi(s)$ is the Mellin transform of the energy distribution of the produced pions (eq.(2)),

$$\phi(s) = \int_0^1 x^s dx \varphi(E_0, E) \quad \left(x = \frac{E}{E_0} \right),$$

and $\langle (1-K)^s \rangle$ is given by

$$\langle (1-K)^s \rangle = \int_0^1 (1-K)^s dK = \frac{1}{s+1}$$

References

- J.N. Capdevielle et al., Preprint of Kernforschungszentrum Karlsruhe KfK 4998 (1992).
M.N. Dyakonov et al., Proc. 20th Int. Cosmic Ray Conf. (Moscow) Vol.6 (1987) 147.
T.K. Gaisser et al, Rev. Mode. Phys. **50** (1978) 859.
T. Hara et al., Phys. Rev. Lett. **50** (1983) 2058.
M. Nagano et al., Preprint of Forschungszentrum Karlsruhe, FZKA 6191 (1998).
R.A. Nam et al., Proc. 18th Int. Cosmic Ray Conf. (Bangalore) Vol.5 (1983)336.
A. Ohsawa, K. Sawayanagi, Phys. Rev. **D49** (1992) 3128-3133.
A. Ohsawa, E.H. Shibuya and M. Tamada, to appear in Phys. Rev. **D**; in this proceedings.